Title

Three-dimensional scapular morphology is associated with rotator cuff tears and alters the abduction moment arm of the supraspinatus

Authors

Lee, Erin CS
Roach, Neil T
Clouthier, Allison L
et al.

Publication Date

2020-08-01

DOI

10.1016/j.clinbiomech.2020.105091

Peer reviewed

HHS Public Access

Author manuscript

Clin Biomech (Bristol, Avon). Author manuscript; available in PMC 2021 May 28.

Published in final edited form as:

Clin Biomech (Bristol, Avon). 2020 August ; 78: 105091. doi:10.1016/j.clinbiomech.2020.105091.

Three-dimensional scapular morphology is associated with rotator cuff tears and alters the abduction moment arm of the supraspinatus

Erin C.S. Lee[a,*], **Neil T. Roach**[b], **Allison L. Clouthier**[c], **Ryan T. Bicknell**[d], **Michael J. Bey**[e], **Nathan M. Young**[f], **Michael J. Rainbow**[a]

[a]Department of Mechanical and Materials Engineering, Queen's University, Kingston, ON, Canada

[b]Department of Human Evolutionary Biology, Harvard University, Cambridge, MA, USA

[c]School of Human Kinetics, University of Ottawa, Ottawa, ON, Canada

[d]Department of Surgery, Kingston Health Sciences Centre, Kingston, Canada

[e]Department of Orthopaedic Surgery, Henry Ford Hospital, Detroit, MI, USA

[f]Department of Orthopaedic Surgery, University of California San Francisco, CA, USA

Abstract

Background: Numerous studies have reported an association between rotator cuff injury and two-dimensional measures of scapular morphology. However, the mechanical underpinnings explaining how these shape features affect glenohumeral joint function and lead to injury are poorly understood. We hypothesized that three-dimensional features of scapular morphology differentiate asymptomatic shoulders from those with rotator cuff tears, and that these features would alter the mechanical advantage of the supraspinatus.

Methods: Twenty-four individuals with supraspinatus tears and twenty-seven age-matched controls were recruited. A statistical shape analysis identified scapular features distinguishing symptomatic patients from asymptomatic controls. We examined the effect of injury-associated morphology on mechanics by developing a morphable model driven by six degree-of-freedom biplanar videoradiography data. We used the model to simulate abduction for a range of shapes and computed the supraspinatus moment arm.

Findings: Rotator cuff injury was associated with a cranial orientation of the glenoid and scapular spine ($P = .011$, d = 0.75) and/or decreased subacromial space ($P = .001$, d = 0.94). The shape analysis also identified previously undocumented features associated with superior inclination and subacromial narrowing. In our computational model, warping the scapula from a

[*]Corresponding author at: Department of Mechanical and Materials Engineering and Human Mobility Research Centre, Queen's University, 130 Stuart Street, Kingston, ON K7L 3N6, Canada., erin.lee@queensu.ca (E.C.S. Lee).

Declaration of Competing Interest

None.

Appendix A. Supplementary data

Supplementary data to this article can be found online at https://doi.org/10.1016/j.clinbiomech.2020.105091.

cranial to a lateral orientation increased the supraspinatus moment arm at 20° of abduction and decreased the moment arm at 160° of abduction.

Interpretations: Three-dimensional analysis of scapular morphology indicates a stronger relationship between morphology and cuff tears than two-dimensional measures. Insight into how morphological features affect rotator cuff mechanics may improve patient-specific strategies for prevention and treatment of cuff tears.

Keywords

Shoulder; Biplanar videoradiography; Statistical shape modeling; Rotator cuff; Musculoskeletal modeling; Imaging - computed tomography

1. Introduction

Full-thickness tears of the rotator cuff (RC) occur in 20–25% of the general population, with incidence increasing substantially with age (Minagawa et al., 2013; Tempelhof et al., 1999; Yamamoto et al., 2010). While the causes of RC tears are undoubtedly multifactorial, (Seitz et al., 2011) numerous studies have reported significant associations between two-dimensional (2D) measures of scapular morphology and RC pathology (Balke et al., 2013; Banas et al., 1995; Bigliani et al., 1986; Cherchi et al., 2016; Flieg et al., 2008; Hughes et al., 2003; Kim et al., 2012; Moor et al., 2013; Moor et al., 2014; Nyffeler et al., 2006; Pandey et al., 2016; Tétreault et al., 2004). Injury-linked morphological features, such as cranial orientation of the glenoid and subacromial narrowing, suggest that glenohumeral instability and/or subacromial impingement play a role. Insight into how these shape features and their associated biomechanics contribute to the development or progression of an RC tear may enable patient-specific preventative and rehabilitation therapies, as well as precise reconstruction surgeries.

While the current 2D measures of scapular morphology, such as the acromion index and critical shoulder angle (CSA), have been shown to differentiate asymptomatic shoulders from those with RC tears, (Balke et al., 2013; Banas et al., 1995; Bigliani et al., 1986; Cherchi et al., 2016; Flieg et al., 2008; Hughes et al., 2003; Kim et al., 2012; Moor et al., 2013; Moor et al., 2014; Nyffeler et al., 2006; Pandey et al., 2016; Tétreault et al., 2004) the shoulder is a complex three-dimensional (3D) joint; therefore, it is difficult to determine how shape features captured by 2D measures alter 3D shoulder biomechanics. Moreover, current 2D measures may not differentiate distinct shape features that contribute to different injury mechanisms. While several studies have found that a larger CSA strongly correlates with RC tears, (Cherchi et al., 2016; Moor et al., 2013; Moor et al., 2014; Pandey et al., 2016) the explanatory utility of the CSA is limited from a biomechanical perspective because it cannot parse whether an individual with a large CSA developed an RC injury from superior glenoid inclination, a laterally extended acromion, an inferiorly positioned acromion, or a combination of each feature.

3D analysis of scapular morphology may provide further insight into the shape-function relationships for two reasons. First, 3D shape analyses, such as statistical shape modeling, isolate features based on how well they capture variation across a population. This allows

features that may be important to the development of an RC tear to be separated from those that are not. Second, 3D shape models provide a continuum of scapular shapes that can be morphed from injured to uninjured forms, allowing for mechanical analyses of disease states (Clouthier et al., 2019). Such variation in scapular morphology across individuals likely introduces variations in the forces and moments and the associated control strategies that are required to maintain the balance among numerous muscle groups. For example, scapular morphology likely influences muscle moment arms – a measure of the muscles' mechanical advantage. Moment arms may be relevant to injury because a muscle with a decreased moment arm must produce a greater stress to generate joint motion. Tendon damage may occur when this greater stress level is repetitively induced throughout activities of daily living. For example, damage to the supraspinatus tendon caused by overuse has been reported in animal studies and in elite athletes (Dischler et al., 2017; Soslowsky et al., 2000). The mechanical advantage of the supraspinatus alters the stress induced to the tendon and could perhaps affect the number of cycles that can be endured before injury occurs.

Previous studies of muscle moment arms have provided insight into shoulder function (Ackland et al., 2008; Gatti et al., 2007; Kuechle et al., 1997; Kuechle et al., 2000; Langenderfer et al., 2006; Liu et al., 1997; Ruckstuhl et al., 2009; Webb et al., 2014). One study found that muscle moment arms were lower for a torn RC compared to an intact RC (Adams et al., 2007). However, there remains a lack of biomechanical evidence to suggest how pre-existing morphological differences in bone shape may increase the likelihood of RC tears. Moreover, current biomechanical studies typically use idealized mechanical models (*e.g.* ball-and-socket models with tendons wrapping over idealized geometry) to examine changes in glenohumeral stability with changes to the CSA (Viehöfer et al., 2016; Gerber et al., 2014; Moor et al., 2016). One computational study used a scapula bone surface model and extended the acromion manually to adjust the CSA (Viehöfer et al., 2015). While these studies inform how the CSA affects the RC activity required to maintain joint stability, incorporating robust 3D changes of scapular morphology based on *in vivo* data may improve our understanding of potential causative mechanisms of RC tears.

The purpose of this study was to 1. identify the 3D morphological differences between asymptomatic controls and individuals with symptomatic full-thickness RC tears and, 2. to determine how changes in scapular shape across individuals affect the mechanical advantage of the supraspinatus muscle. We introduce an approach to determine muscle moment arms as a function of both kinematics and shape using a combination of statistical shape modeling, contact modeling, and muscle fibre wrapping. The approach is validated using accurate biplanar videoradiography data (Bey et al., 2009). Consistent with the CSA, we hypothesized that scapula shapes associated with RC tears would display decreased subacromial space and increased superior inclination of the glenoid and that these changes would decrease the abduction moment arm of the supraspinatus.

2. Methods

2.1. Data collection

Following IRB approval and informed consent, individuals with MRI-diagnosed, chronic, full thickness supraspinatus tears (n = 24, mean age = 60.2 years, 7 males and 17 females)

and age-matched controls with no history of RC pathology (n = 27, mean age = 58.7 years, 7 males and 20 females) were recruited. The shoulder complex was CT scanned (GE Medical Systems, LightSpeed16, Piscataway, New Jersey, USA) and the humerus and scapula were isolated from other bones and soft tissue using a semiautomatic segmentation technique (Mimics 10.1, Materialise, Leuven, Belgium). This yielded three-dimensional tessellated surface meshes of the humerus and scapula. Each subject was asked to abduct their shoulder from approximately 0° to 120° in the coronal plane while biplanar videoradiography was captured (60 Hz). Six degree-of-freedom kinematics of the humerus and scapula were obtained using a markerless registration technique with previously reported errors within 0.39 mm and 0.47° (Bey et al., 2006). This error implicitly considers the accuracy of the segmentation and reconstruction process. Bey et al. previously reported an analysis relating 3D kinematics to 2D measures such as CSA using a subset of these data (Bey et al., 2009; Bishop et al., 2009).

2.2. Landmark data

For each individual we first recorded the 3D coordinates of 29 anatomical landmarks on each scapula surface model (Supplemental S1). These landmarks were chosen to capture the shape of the body, glenoid, spine, acromion, and coracoid process and are based on standards in comparative morphology (Young, 2004; Young, 2006; Young et al., 2015). The landmarks were placed by a single user using a semiautomated user-directed method in the software *Landmark Editor 3.6* (IDAV, Davis, CA, USA). Shape was quantified using three-dimensional geometric morphometrics (Zelditch et al., 2012). First, the raw 3D coordinates for each scapula were aligned and scaled to a common centroid size and rotated to minimize distance *via* generalized Procrustes superimposition as implemented in the *R* statistical software package *geomorph* (R Foundation for Statistical Computing, Vienna, Austria). We further tested for and removed the effects of allometry (size:shape relationships) by regressing against centroid size and utilizing the computed residuals.

2.3. Shape analysis

We applied Principal Components Analysis (PCA) to the 3D Procrustes coordinates to identify correlated morphological changes that explain the largest proportion of total shape variation. PCA was performed on the 3D (x,y,z) coordinates of the anatomical landmarks following Procrustes superimposition. Briefly, PCA identifies axes (principal components or PCs) that explain successively smaller amounts of variation (eigenvalues) described as suites of covarying shape changes (the corresponding eigenvector). Importantly, no *a priori* assumption is made concerning group structure, thus 3D coordinates were pooled from both groups and any separation is of special interest. The algorithm for this shape analysis (Supplemental S2) has been previously applied in several biomechanics studies (Bredbenner et al., 2010; Cootes et al., 1995; Haverkamp et al., 2011; Clouthier et al., 2019). Unpaired *t*-tests were performed to determine which PCs significantly differentiate mean scapula shape of RC tears from asymptomatic controls. The level of significance was set to 5%. Cohen's effect size was then computed for each PC.

2.4. Biomechanical model

Subsequent biomechanical modeling was performed on reconstructions of scapula surface models that linearly spanned the range of each principal component. For each PC that significantly differentiated RC tears from controls, 3D models were generated by applying the associated eigenvector to the calculated mean shape of the population spanning PC scores from the extremes of the observed distributions (Supplemental S2). Models generated from the associated PC were assigned normalized values from −10 to +10, producing 21 models for each PC.

To examine the effect of shape on mechanical advantage of the muscles, we developed a morphable, congruence-based musculoskeletal model that could be automatically applied to any set of humerus and scapula bone shapes and driven through any physiological shoulder motion. Using one subject's scapula and humerus as a template model, we manually plotted muscle and ligament insertion sites to the template meshes based on anatomical texts (Grant, 1972; Primal Pictures Ltd., 2006). Coherent Point Drift was used to establish correspondence among surface vertices across all 21 scapulae (Myronenko and Song, 2010). The insertion sites were automatically assigned to vertices that corresponded to the same anatomical landmarks across all reconstructed scapulae (Clouthier et al., 2019).

To isolate the effects of scapular morphology, the scaled template humerus was paired with all scaled scapula shape models. Each muscle and ligament was represented as 2–3 individual fibres, with each fibre modelled as a string of 40 points (Fig. 1). In each glenohumeral joint pose, the points were optimized such that each fibre traversed the shortest distance from origin to insertion, with the constraint that the fibre could not penetrate the bone surfaces (Marai et al., 2004).

2.5. Data-driven kinematic simulation

The *in vivo* kinematics during the abduction task were variable across subjects with out-of-plane rotations ranging from 0° to 51°. To isolate shape features as the independent variable, we specified an abduction task with identical rotational kinematics across all models, while allowing the translational degrees-of-freedom to vary for each model such that congruence between the glenoid and humerus was maximized. The optimization favoured an average distance between the humeral head and glenoid fossa that reflected the distances observed in the asymptomatic subjects' *in vivo* kinematic data. This approach effectively approximates cartilage contact and assumes that no shoulder instabilities are present (Supplemental S3).

The specified kinematic path was informed by the *in vivo* biplanar videoradiography data of the asymptomatic subjects. Anatomical coordinate systems were computed and glenohumeral joint angles were calculated using a Y-*Z*-Y Euler rotation between humeral and scapular coordinate systems in accordance with ISB recommendations (Wu et al., 2005). Thoracohumeral abduction was calculated using the Y-Z-Y Euler rotation sequence between the humeral coordinate system and the fixed global coordinate system, assuming the motion of the thorax was negligible (Supplemental S4–S5). To determine the corresponding elevation plane angle and axial rotation angle, we identified three subjects that performed abduction with minimal motion in the transverse plane of the scapula. We used linear and

quadratic regression (Matlab, 2016) to obtain the elevation plane and axial rotation angles, respectively, that best fit the collected data (Fig. 2). The best-fit joint angles were used to simulate motion for a full range of abduction from 0° to 160°. Abduction was simulated using these specified rotational kinematics and the congruence constraint for each reconstructed model spanning the PCs that differentiated the groups. (See Fig. 3.)

2.6. Moment arm calculation

We calculated the supraspinatus moment arm across simulated abduction using the geometric method, which estimates the tendency of a muscle to rotate the humerus about the instantaneous helical axis (Supplemental S6) (Pandy, 1999). The supraspinatus moment arm was calculated based on the middle fibre, as it represented an average of the three modelled fibres.

Shoulder motion and muscle fibres were simulated for scapular geometries spanning each significant principal component (PC). The computed moment arms were plotted as a function of abduction, as well as shape at three specific thoracohumeral abduction angles: 20°, 90°, and 160°. These angles were chosen to determine the supraspinatus mechanical advantage for activities at low, medium, and high abduction angles. Linear regression was performed on moment arm as a function of shape at each of the targeted abduction angles for each significant PC. An F-test determined if the slope was non-zero using the 5% level of significance and R^2 values quantified goodness-of-fit, (Graphpad Prism, San Diego, California).

3. Results

3.1. Shape analysis

The first four Principal Components (PCs) captured 49.7% of the shape variation in the dataset (Fig. 4). Two principal components, Principal Component 2 (PC2) and PC4 significantly discriminated the asymptomatic and tear groups with P values of $P = .011$ and $P = .001$ respectively (Figs. 4,5). PC1 and PC3 were not significantly different between groups ($P = .760$ and 0.612, respectively) (Fig. 4). Cohen's effect size values were strong for PC2 and PC4 (d = 0.75 and d = 0.94, respectively) and weak for PC1 and PC3 (d = 0.086 and d = 0.14, respectively).

The PC2 shape axis was primarily associated with a coordinated change in glenoid and scapular spine orientation from cranial (negative) to lateral (positive). Simultaneously, the inferior region of the subscapular fossa, which is the attachment site for the teres major, widened and shifted to a more superior orientation (Fig. 5b). The PC4 shape axis was associated with a superior and medially retracted shift of the acromion, a posterior rotation of the coracoid process, and an anterior-posterior narrowing of the supraspinous fossa (Fig. 5d). The glenoid also shifted from retroverted to anteverted, with an 8.7° change in glenoid version angle across the extremes of the sampled scores. Together these PC4 changes described relative opening of the subacromial space due to the superior shift in the acromion. Animations visualizing these shape changes are provided in the supplemental material.

3.2. Supraspinatus moment arms

The supraspinatus moment arm for the mean scapula shape decreased from approximately 20.8 mm to 8.3 mm as the humerus was abducted from 0° to 160° (Fig. 6), corresponding to a change throughout the motion of 60% of the maximum moment arm. The supraspinatus moment arm remained relatively constant for the first 100° of abduction, decreasing by 0.8 mm, before decreasing rapidly at higher abduction angles.

The supraspinatus moment arms were significantly affected by PC2 (Fig. 7a) at all levels of abduction ($P < .001$, $R^2 > 0.86$). Warping the scapula from a cranial orientation to a lateral orientation increased the supraspinatus moment arm at 20° of abduction (+2.4 mm) but decreased the moment arm at 160° (−4.4 mm). The effect of shape on moment arm at 90° was statistically significant but comparatively small (+0.5 mm) as the supraspinatus moment arm slightly increased from cranial to lateral orientation.

The supraspinatus moment arms were also significantly affected by PC4 (Fig. 7b) at all levels of abduction ($P = .013$ at 20°, $P = .002$ at 90°, $P = .021$ at 160°, $0.25 < R^2 < 0.45$), however the moment arm changes were smaller in magnitude than the changes due to PC2. Increasing the subacromial space and narrowing the supraspinous fossa increased the supraspinatus moment arm at 20° of abduction (+0.4 mm) and 90° of abduction (+0.4 mm) but decreased the moment arm at 160° (−0.9 mm).

4. Discussion

We coupled statistical shape analysis to a congruence-based biomechanical model to investigate the relationships between supraspinatus pathology, scapular morphology, and muscle mechanical advantage. Our data-driven approach was guided by three-dimensional bone surface models and accurate *in vivo* six-degree-of-freedom shoulder kinematics acquired with biplanar videoradiography. As hypothesized, cranial orientation of the glenoid and subacromial narrowing were both strongly associated with RC tears. Biomechanical analysis of these shape features revealed that from 0°–160° of thoracohumeral abduction, cranial orientation decreased the supraspinatus moment arm at low levels of abduction as hypothesized but increased the moment arm at high levels of abduction. The shape analysis also revealed new features associated with supraspinatus tears.

The PCA served as a post-hoc analysis to identify shape features that explained the greatest variation between RC tears and controls. Cranial orientation (PC2) was strongly associated with RC tears and explained a greater variation in scapular shape than subacromial narrowing (PC4); however, subacromial narrowing more strongly discriminated scapulae with RC tears from controls. This indicates that the tolerance for injury may be lower for specific but subtle changes in scapular morphology, and confirms previous reports that highlight the importance of morphology in RC pathology (Balke et al., 2013; Banas et al., 1995; Bigliani et al., 1986; Cherchi et al., 2016; Flieg et al., 2008; Hughes et al., 2003; Kim et al., 2012; Moor et al., 2013; Moor et al., 2014; Nyffeler et al., 2006; Pandey et al., 2016). Our data suggest that some individuals possibly develop tears because of scapular morphology captured by PC2, PC4, or a combination of both (Fig. 4a). This result highlights

that there may be different mechanical pathways that can lead to the development of an RC tear.

In contrast to 2D measures of scapular morphology reported in radiographic studies, our 3D shape analysis demonstrated a strong relationship between scapular morphology and RC tears. Previously, several 2D measures of scapular morphology that are associated with RC injury were identified from manual identification of three or four landmarks on 2D radiographs; however, the relationships reported across these are often weak and inconsistent (Balke et al., 2013; Banas et al., 1995; Bigliani et al., 1986; Flieg et al., 2008; Hughes et al., 2003; Kim et al., 2012; Moor et al., 2014; Pandey et al., 2016; Tétreault et al., 2004). The inconsistency in 2D studies may be due, in part, to limitations of projecting the complex 3D shape of the scapula onto a plane. Our robust 3D shape analysis incorporates 29 landmarks capturing the complexity of scapular morphology. Additionally, our shape analysis captured previously undocumented features that were associated with cranial orientation and subacromial narrowing. For example, as the glenoid became more cranial, the teres major attachment site decreased in size and shifted to a lateral orientation (PC2). Moreover, as the subacromial space narrowed, the supraspinous fossa widened and the glenoid shifted to an anteverted orientation (PC4). These features are not captured in the existing 2D measures, which highlights the importance of performing 3D analyses of scapular morphology.

The strong association between subacromial narrowing (PC4) and RC tears may support the widely accepted theory of impingement as a cause of supraspinatus tears (Neer, 1972; Neer, 1983) PC4 shows a simultaneous lateral extension and inferior shift of the acromion, which is consistent with 2D measures reported in radiographic studies (Balke et al., 2013; Kim et al., 2012; Moor et al., 2014; Nyffeler et al., 2006; Pandey et al., 2016). As hypothesized, superior inclination of the glenoid (PC2) was strongly correlated with RC tears; however, three-dimensional shape analysis captured a simultaneous superior inclination of the scapular spine which effectively maintains a constant subacromial space. The PCA indicates that the orientation of the glenoid tends to remain in parallel with the scapular spine but shifts to a cranial inclination relative to the scapula’s medial border. Current measures of glenoid inclination, including the CSA, measure the glenoid relative to the scapular spine or acromion (Bishop et al., 2009; Hughes et al., 2003; Kandemir et al., 2006; Moor et al., 2013). This could explain the inconsistency in literature reporting the association between glenoid inclination angle and RC tears, as these 2D angles could be falsely quantifying changes in acromion curvature or scapular spine shape as changes to the inclination angle.

Our investigation elucidates a potential mechanism for injury explained by scapular morphology. The effect of cranial orientation of the glenoid (PC2) on the muscles’ mechanical advantage (Fig. 7) implies that the reduced mechanical advantage of the supraspinatus in cranialized scapulae at low levels of abduction would increase the force required by the supraspinatus to abduct the arm, thus increasing stress in the tendon. It is possible that repetitive abduction motions below 90° with this elevated stress may increase susceptibility to supraspinatus tears in individuals with cranially oriented scapulae. This is especially significant when considering most activities of daily living involve abduction below 90° (Aizawa et al., 2010). The evolutionary literature supports this hypothesis. Throughout human evolutionary history the glenoid has become increasingly lateralized,

presumably due to selective pressures for tasks with lower abduction such as throwing, digging, or tool use (Harmand et al., 2015; Hunt, 1991; McPherron et al., 2010; Roach et al., 2013; Skinner et al., 2015; Young et al., 2015). The increased mechanical advantage of the supraspinatus for cranial scapulae above 90° of abduction may reduce its force requirement and increase power for activities in this range when compared to laterally oriented scapulae. However, repetitive overhead tasks are generally less common in modern humans today.

Variation in the supraspinatus moment arm as a function of shape may alter the load requirements of other RC muscles. For example, a cadaveric study reported that increasing supraspinatus strain and tear size increased the maximum strain to the infraspinatus and suggested that the infraspinatus tendon may play a stress shielding role to minimize the risk of supraspinatus tear propagation (Andarawis-Puri et al., 2009). This could explain why 18% of supraspinatus tears are accompanied by infraspinatus tears (Minagawa et al., 2013). It is possible that for cranially oriented scapulae, at abduction below 90°, the infraspinatus tendon must supply an increased load to accommodate the reduced mechanical advantage of the supraspinatus in abduction.

The magnitude of change in the moment arm caused by glenoid orientation (PC2) was approximately five-fold greater than the change caused by subacromial space (PC4) (Fig. 7). These results suggest that decreasing the subacromial space does not affect the supraspinatus moment arm in a way that would influence its mechanical advantage during abduction. This is unsurprising given changes in subacromial space are thought to be more important for impingement of the supraspinatus tendon (Balke et al., 2013). Further, the glenoid version also explained by PC4 may have an impact on joint stability and contact force that is not captured by the supraspinatus abduction moment arm or our current model.

We computed moment arms only for morphological changes associated with injury; however, we recognize that other morphological factors, such as the striking difference in scapular body aspect ratio observed in PC1, may alter moment arms. Given that this feature explains a quarter of the variation in the dataset, we postulate that simultaneous changes to humerus morphology compensate for changes to scapular morphology to regulate the moment arm. Conversely, it is less likely that humerus morphology can compensate for moment arm changes caused by cranial orientation alone. Further statistical shape analysis and musculoskeletal modeling must be performed at the glenohumeral joint level to confirm this theory.

To help validate our model, we compared our moment arm results to reported values in the literature. The literature regarding abduction moment arms is variable due to the different techniques used for data collection and moment arm calculation, (Ackland et al., 2008; Gatti et al., 2007; Kuechle et al., 1997; Liu et al., 1997; Ruckstuhl et al., 2009; Webb et al., 2014) making it challenging to compare specific moment arm values and moment arm curves across studies. We found that RC moment arms were highly sensitive to small changes in kinematics, indicating that the general inconsistency across moment arm studies may also be due to differences in the defined abduction kinematics. To address this, our moment arm analysis used accurate *in vivo* kinematic data to estimate the glenohumeral joint angles associated with isolated thoracohumeral abduction, which allowed us to account for the

scapular rotation, scapular tilt, and axial rotation of the humerus that naturally occur during *in vivo* abduction (Supplemental S7). Therefore, we were able to simulate motion that is more realistic than idealized in-plane abduction. Our computed range of the supraspinatus moment arm from 0° to 160° abduction is consistent with the results of previous cadaveric experiments (Ackland et al., 2008; Kuechle et al., 1997; Liu et al., 1997) and computational studies (Ruckstuhl et al., 2009; Webb et al., 2014). Further, most moment arm studies have reported a negative trend in the supraspinatus moment arm with increasing abduction angle, and our results support these findings (Ackland et al., 2008; Kuechle et al., 1997; Webb et al., 2014).

Our study had several limitations. First, the experiment had a cross-sectional design, making it impossible to distinguish cause from effect. However, the shape of the scapula is formed early during development (Young, 2006) and it is therefore unlikely that the substantial morphological changes we observed are secondary to the onset of an RC tear. Second, the current musculoskeletal model limits muscle representation to individual fibres with single insertion and origin points even though the RC muscles attach over wider regions. We selected points at the centre of each insertion region as a representation of the muscle's average line-of-action. Further, there are other mechanical factors, such as lines of action and muscle-tendon stress, that were not captured by our model and are likely important to pathomechanics. Building on our approach will allow these factors to be investigated in future studies.

The present study has identified shape features that go beyond the acromion- and glenoid-focused radiographic measures currently used in the literature. The supraspinatus mechanical advantage was most affected by the simultaneous cranial orientation of the glenoid and scapular spine, which is not captured by the current 2D measures. This indicates the need for improved morphological measures for predicting changes in muscle mechanics. We recognize that using a robust statistical shape model requires extensive segmentation and computation time and it may not always be feasible to acquire 3D surface models. The complex shape features identified here could be used to develop more sensitive 2D measures that incorporate the previously unreported features. These new 2D measures could augment the current 2D radiographic measures for identifying patients with "at-risk" shoulder morphology and informing treatment.

It should be noted that despite identifying statistical differences in specific scapula between injured and asymptomatic individuals, the morphological features were not completely distinct between the two groups. Although it is less common, there were asymptomatic individuals that have "at-risk" scapula features such as a cranial glenoid and small subacromial space, and individuals with RC tears who have scapula features associated with the asymptomatic group. We postulate two possible reasons for the occurrence of asymptomatic individuals with "at-risk" shapes. First, since we found the moment arms were highly sensitive to small changes in kinematics, it is possible that individuals adapt their kinematics given their scapula morphology to optimize muscle moment arms; for example, individuals may adopt unique activation patterns and/or alter their scapulothoracic kinematics. It is possible that asymptomatic individuals with "at-risk" scapula features use kinematics that are optimal for their scapula morphology and thus avoid injury. Indeed,

scapular morphology may partially explain discrepancies in the literature around supraspinatus activation patterns (Escamilla et al., 2009; Favre, 2012; Reed et al., 2013). If there is an optimal kinematic path associated with each shoulder shape, then clinicians may be able to design subject-specific therapies to prevent injury. Future work is required to investigate this idea. Second, given that most activities of daily living do not involve tasks that load the shoulder, (Aizawa et al., 2010) individuals with "at-risk" shapes may avoid injury because they do not frequently perform activities that induce stress on the supraspinatus tendon.

5. Conclusions

We identified novel shape changes associated with RC tears, including the orientation of the glenoid and scapular spine, that are associated with RC tears and affect the supraspinatus mechanical advantage when kinematics are controlled. This study introduces a framework that can match any scapula shape with any set of joint kinematics and measure the mechanical advantage of the rotator cuff muscles as a function of morphology. This framework could be used to consider patient-specific shape to predict the mechanical outcomes of surgical interventions such as supraspinatus tendon repair. Furthermore, matching mechanics with shape may facilitate better preventative and rehabilitation strategies, as clinicians may be able to retrain patients to move their shoulders in a manner that is optimal for their skeletal shape.

Supplementary Material

Refer to Web version on PubMed Central for supplementary material.

Funding

This work was funded in part by the Natural Sciences and Engineering Research Council of Canada and the National Science Foundation [BCS-1518596].

References

Ackland DC, Pak P, Richardson M, Pandy MG, 2008. Moment arms of the muscles crossing the anatomical shoulder. J. Anat 213, 383–390. [PubMed: 18691376]

Adams CR, Baldwin MA, Laz PJ, Rullkoetter PJ, Langenderfer JE, 2007. Effects of rotator cuff tears on muscle moment arms: a computational study. J. Biomech 40, 3373–3380. [PubMed: 17597135]

Aizawa J, et al., 2010. Three-dimensional motion of the upper extremity joints during various activities of daily living. J. Biomech 43, 2915–2922. [PubMed: 20727523]

Andarawis-Puri N, Ricchetti ET, Soslowsky LJ, 2009. Interaction between the supraspinatus and infraspinatus tendons: effect of anterior supraspinatus tendon full-thickness tears on infraspinatus tendon strain. Am. J. Sports Med 37, 1831–1839. [PubMed: 19483078]

Balke M, et al., 2013. Correlation of acromial morphology with impingement syndrome and rotator cuff tears. Acta Orthop 84, 178–183. [PubMed: 23409811]

Banas MP, Miller RJ, Totterman S, 1995. Relationship between the lateral acromion angle and rotator cuff disease. J. Shoulder Elb. Surg 4, 454–461.

Bey MJ, Zauel R, Brock SK, Tashman S, 2006. Validation of a new model-based tracking technique for measuring three-dimensional, in vivo glenohumeral joint kinematics. J. Biomech. Eng 128, 604–609. [PubMed: 16813452]

Bey MJ, Kline SK, Zauel R, Kolowich PA, Lock TR, 2009. In vivo measurement of Glenohumeral joint contact patterns. EURASIP J. Adv. Signal Process 2010 (162136).

Bigliani LU, Morrison DS, April EW, 1986. The morphology of the acromion and its relationship to rotator cuff tears. Orthop. Trans 10, 228.

Bishop JL, Kline SK, Aalderink KJ, Zauel R, Bey MJ, 2009. Glenoid inclination: in vivo measures in rotator cuff tear patients and associations with superior glenohumeral joint translation. J. Shoulder Elb. Surg 18, 231–236.

Bredbenner TL, et al., 2010. Statistical shape modeling describes variation in tibia and femur surface geometry between control and incidence groups from the osteoarthritis initiative database. J. Biomech 43, 1780–1786. [PubMed: 20227696]

Cherchi L, Ciornohac JF, Godet J, Clavert P, Kempf J-F, 2016. Critical shoulder angle: measurement reproducibility and correlation with rotator cuff tendon tears. Orthop. Traumatol. Surg. Res 102, 559–562. [PubMed: 27238292]

Clouthier AL, et al., 2019. The effect of articular geometry features identified using statistical shape modelling on knee biomechanics. Med. Eng. Phys 66, 47–55. [PubMed: 30850334]

Cootes TF, Taylor CJ, Cooper DH, Graham J, 1995. Active shape models-their training and application. Comput. Vis. Image Underst 61, 38–59.

Dischler JD, Baumer TG, Finkelstein E, Siegal DS, Bey MJ, 2017. Association between years of competition and shoulder function in collegiate swimmers. Sports Health 10, 113–118. [PubMed: 28829699]

Escamilla RF, Yamashiro K, Paulos L, Andrews JR, 2009. Shoulder muscle activity and function in common shoulder rehabilitation exercises. Sports Med. Auckl. NZ 39, 663–685.

Favre P, et al., 2012. An integrated model of active glenohumeral stability. J. Biomech 45, 2248–2255. [PubMed: 22818663]

Flieg NG, et al., 2008. A stochastic analysis of glenoid inclination angle and superior migration of the humeral head. Clin. Biomech 23, 554–561.

Gatti CJ, Dickerson CR, Chadwick EK, Mell AG, Hughes RE, 2007. Comparison of model-predicted and measured moment arms for the rotator cuff muscles. Clin. Biomech 22, 639–644.

Gerber C, Snedeker JG, Baumgartner D, Viehöfer AF, 2014. Supraspinatus tendon load during abduction is dependent on the size of the critical shoulder angle: a biomechanical analysis. J. Orthop. Res. Off. Publ. Orthop. Res. Soc 32, 952–957.

Grant JCB, 1972. Grant's Atlas of Anatomy. The Williams & Wilkins Company.

Harmand S, et al., 2015. 3.3-million-year-old stone tools from Lomekwi 3, West Turkana, Kenya. Nature 521, 310–315. [PubMed: 25993961]

Haverkamp DJ, Schiphof D, Bierma-Zeinstra SM, Weinans H, Waarsing JH, 2011. Variation in joint shape of osteoarthritic knees. Arthritis Rheum 63, 3401–3407. [PubMed: 21811994]

Hughes RE, et al., 2003. Glenoid inclination is associated with full-thickness rotator cuff tears. Clin. Orthop 407, 86–91.

Hunt KD, 1991. Positional behavior in the Hominoidea. Int. J. Primatol 12, 95–118.

Kandemir U, Allaire RB, Jolly JT, Debski RE, McMahon PJ, 2006. The relationship between the orientation of the glenoid and tears of the rotator cuff. J. Bone Joint Surg. (Br.) 88, 1105–1109. [PubMed: 16877616]

Kim JR, Ryu KJ, Hong IT, Kim BK, Kim JH, 2012. Can a high acromion index predict rotator cuff tears? Int. Orthop 36, 1019–1024. [PubMed: 22310972]

Kuechle DK, Newman SR, Itoi E, Morrey BF, An K-N, 1997. Shoulder muscle moment arms during horizontal flexion and elevation. J. Shoulder Elb. Surg 6, 429–439.

Kuechle DK, et al., 2000. The relevance of the moment arm of shoulder muscles with respect to axial rotation of the glenohumeral joint in four positions. Clin. Biomech 15, 322–329.

Langenderfer JE, Patthanacharoenphon C, Carpenter JE, Hughes RE, 2006. Variation in external rotation moment arms among subregions of supraspinatus, infraspinatus, and teres minor muscles. J. Orthop. Res 24, 1737–1744. [PubMed: 16779813]

Liu J, Hughes R, Smutz W, Niebur G, Nan-An K, 1997. Roles of deltoid and rotator cuff muscles in shoulder elevation. Clin. Biomech 12, 32–38.

Marai GE, et al., 2004. Estimating joint contact areas and ligament lengths from bone kinematics and surfaces. IEEE Trans. Biomed. Eng 51, 790–799. [PubMed: 15132505]

McPherron SP, et al., 2010. Evidence for stone-tool-assisted consumption of animal tissues before 3.39 million years ago at Dikika, Ethiopia. Nature 466, 857–860. [PubMed: 20703305]

Minagawa H, et al., 2013. Prevalence of symptomatic and asymptomatic rotator cuff tears in the general population: from mass-screening in one village. J. Orthop 10, 8–12. [PubMed: 24403741]

Moor BK, Bouaicha S, Rothenfluh DA, Sukthankar A, Gerber C, 2013. Is there an association between the individual anatomy of the scapula and the development of rotator cuff tears or osteoarthritis of the glenohumeral joint?: a radiological study of the critical shoulder angle. Bone Jt. J 95–B, 935–941.

Moor BK, Wieser K, Slankamenac K, Gerber C, Bouaicha S, 2014. Relationship of individual scapular anatomy and degenerative rotator cuff tears. J. Shoulder Elb. Surg 23, 536–541.

Moor BK, et al., 2016. Inclination-dependent changes of the critical shoulder angle significantly influence superior glenohumeral joint stability. Clin. Biomech 32, 268–273.

Myronenko A, Song X, 2010. Point set registration: coherent point drift. IEEE Trans. Pattern Anal. Mach. Intell 32, 2262–2275. [PubMed: 20975122]

Neer CS, 1972. Anterior acromioplasty for the chronic impingement syndrome in the shoulder: a preliminary report. J. Bone Joint Surg. Am 54, 41–50. [PubMed: 5054450]

Neer CS, 1983. Impingement lesions. Clin. Orthop 70–77. [PubMed: 6825348]

Nyffeler RW, Werner CML, Sukthankar A, Schmid MR, Gerber C, 2006. Association of a large lateral extension of the acromion with rotator cuff tears. J. Bone Jt. Surg 88, 800–805.

Pandey V, et al., 2016. Does scapular morphology affect the integrity of the rotator cuff? J. Shoulder Elb. Surg 25, 413–421.

Pandy MG, 1999. Moment arm of a muscle force. Exerc. Sport Sci. Rev 27, 79–118. [PubMed: 10791015]

Primal Pictures Ltd., 2006. Anatomy. TV. Primal Pictures Limited.

Reed D, Cathers I, Halaki M, Ginn K, 2013. Does supraspinatus intitiate shoulder abduction? J Electromyogr Kinesiol 23, 425–429. [PubMed: 23265661]

Roach NT, Venkadesan M, Rainbow MJ, Lieberman DE, 2013. Elastic energy storage in the shoulder and the evolution of high-speed throwing in homo. Nature 498, 483–486. [PubMed: 23803849]

Ruckstuhl H, et al., 2009. Shoulder abduction moment arms in three clinically important positions. J. Shoulder Elb. Surg 18, 632–638.

Seitz AL, McClure PW, Finucane S, Boardman ND, Michener LA, 2011. Mechanisms of rotator cuff tendinopathy: intrinsic, extrinsic, or both? Clin. Biomech 26, 1–12.

Skinner MM, et al., 2015. Human-like hand use in Australopithecus africanus. Science 347, 395–399. [PubMed: 25613885]

Soslowsky LJ, et al., 2000. Neer award 1999: overuse activity injures the supraspinatus tendon in an animal model: a histologic and biomechanical study. J. Shoulder Elb. Surg 9, 79–84.

Tempelhof S, Rupp S, Seil R, 1999. Age-related prevalence of rotator cuff tears in asymptomatic shoulders. J. Shoulder Elb. Surg 8, 296–299.

Tétreault P, Krueger A, Zurakowski D, Gerber C, 2004. Glenoid version and rotator cuff tears. J. Orthop. Res 22, 202–207. [PubMed: 14656681]

Viehöfer AF, Gerber C, Favre P, Bachmann E, Snedeker JG, 2015. A larger critical shoulder angle requires more rotator cuff activity to preserve joint stability. J. Orthop. Res 34, 961–968. [PubMed: 26572231]

Viehöfer AF, Snedeker JG, Baumgartner D, Gerber C, 2016. Glenohumeral joint reaction forces increase with critical shoulder angles representative of osteoarthritis-a biomechanical analysis. J. Orthop. Res 34, 1047–1052. [PubMed: 26638117]

Webb JD, Blemker SS, Delp SL, 2014. 3D finite element models of shoulder muscles for computing lines of actions and moment arms. Comput. Methods Biomech. Biomed. Eng 17, 829–837.

Wu G, et al., 2005. ISB recommendation on definitions of joint coordinate systems of various joints for the reporting of human joint motion—part II: shoulder, elbow, wrist and hand. J. Biomech 38, 981–992. [PubMed: 15844264]

Yamamoto A, et al., 2010. Prevalence and risk factors of a rotator cuff tear in the general population. J. Shoulder Elb. Surg 19, 116–120.

Young N, 2004. Modularity and integration in the hominoid scapula. J. Exp. Zool. B Mol. Dev. Evol 302B, 226–240.

Young NM, 2006. Function, ontogeny and canalization of shape variance in the primate scapula. J. Anat 209, 623–636. [PubMed: 17062020]

Young NM, Capellini TD, Roach NT, Alemseged Z, 2015. Fossil hominin shoulders support an African ape-like last common ancestor of humans and chimpanzees. Proc. Natl. Acad. Sci 112, 11829–11834. [PubMed: 26351685]

Zelditch ML, Swiderski DL, Sheets HD, 2012. Geometric Morphometrics for Biologists: A Primer. Academic Press.

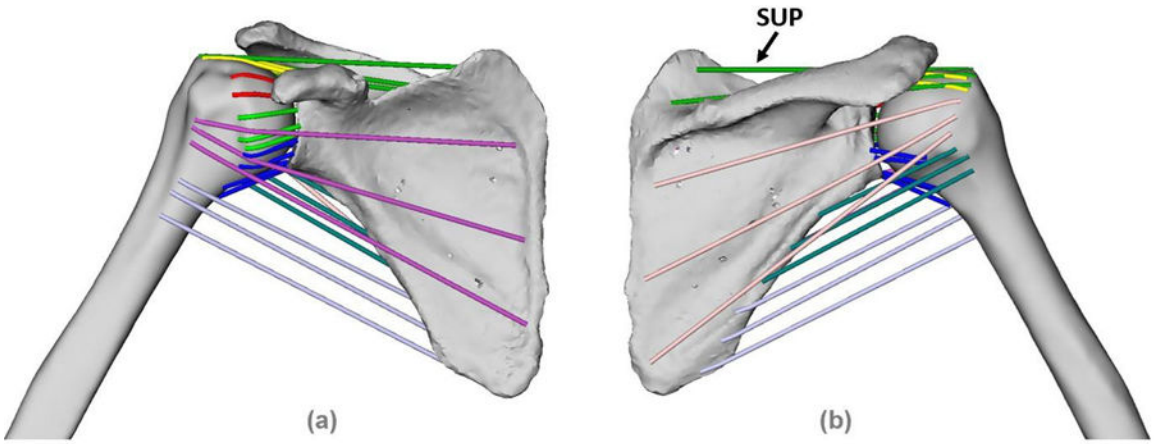

Fig. 1.

(a) Anterior and (b) Posterior view of the musculoskeletal model. Fibres are modelled as a string of 40 points, optimized such that each fibre traversed the shortest distance from origin to insertion without penetrating the bone surface. The origin and insertion points were automatically mapped to all generated shape models and muscle fibres were calculated for each frame of the kinematic data. The supraspinatus (SUP) fibres are labelled.

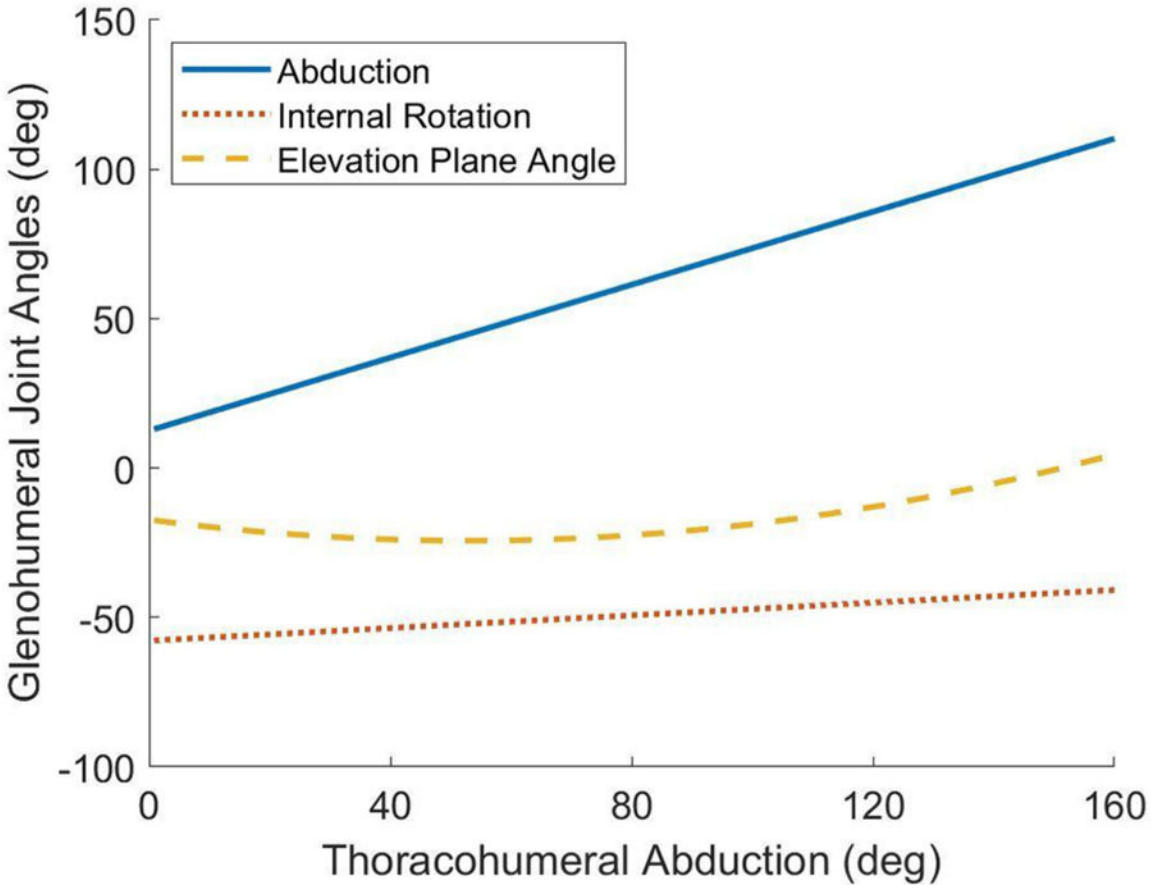

Fig. 2.

The glenohumeral joint angles for 160 degrees of thoracohumeral abduction. The abduction and internal rotation angles were determined from the linear fit to subject *in vivo* kinematic data and the elevation plane angle was determined from a quadratic fit to the *in vivo* data.

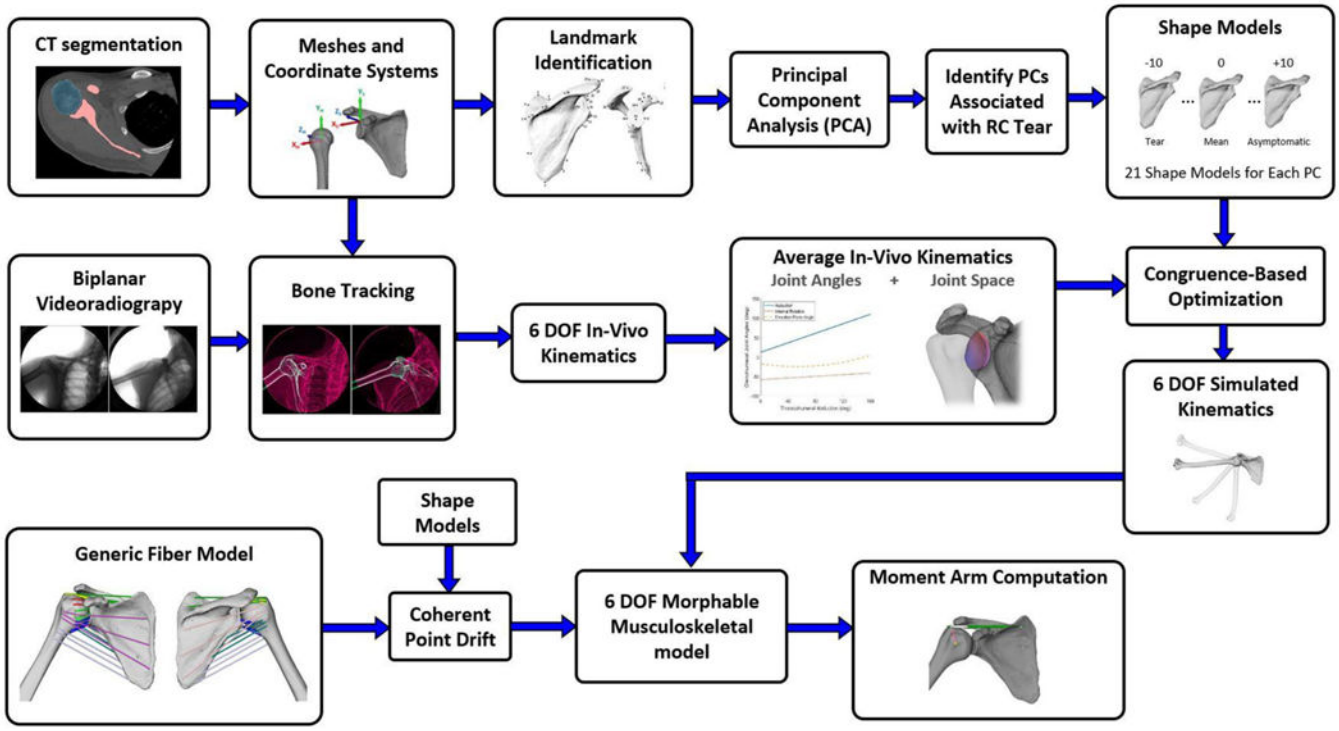

Fig. 3.

Overview of the methodology including data acquisition, data processing, and shape and biomechanical analyses.

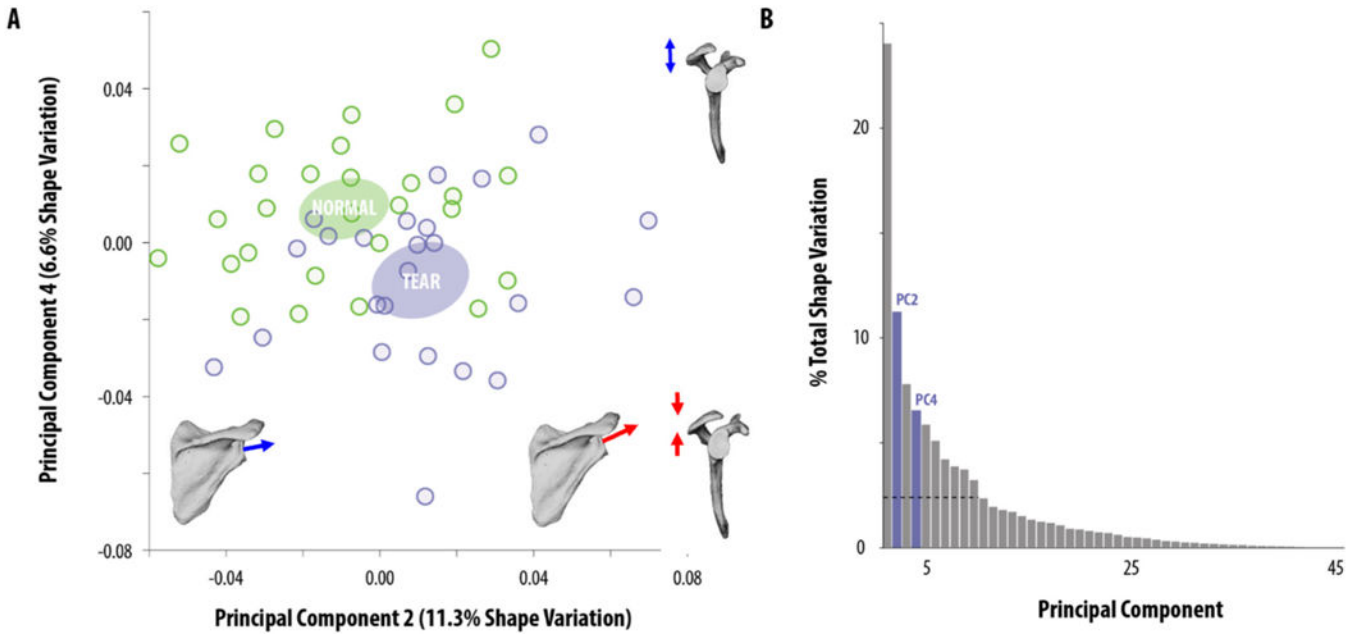

Fig. 4.

(a) Scatter plot of PC4 *vs.* PC2 scores for asymptomatic subjects and subjects with full thickness supraspinatus tears. (b) Variation explained by each PC.

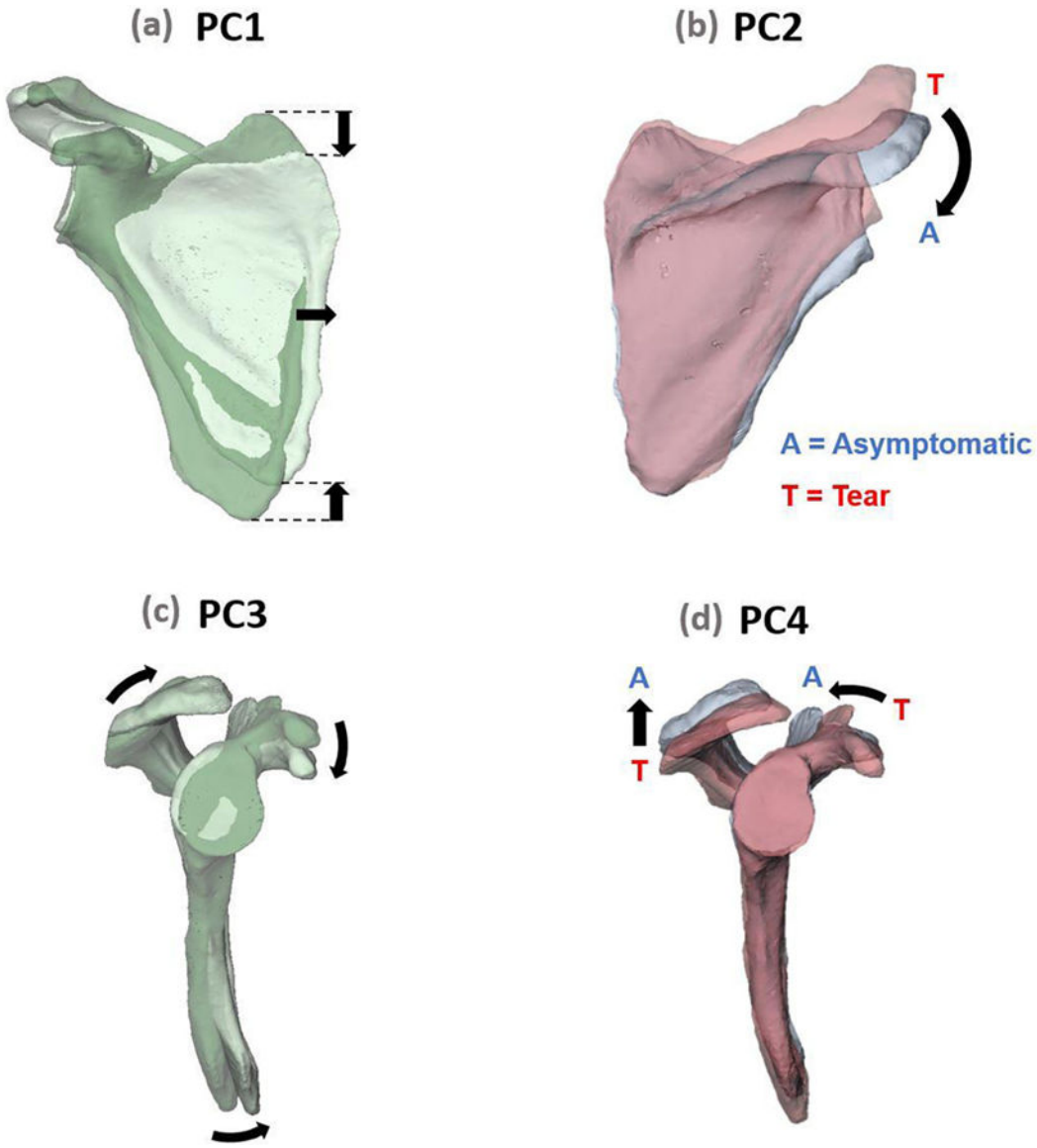

Fig. 5.

The first four principal components describe the greatest modes of variation in the dataset. PC2 and PC4 significantly distinguished the asymptomatic and tear subjects, while PC1 and PC3 did not. (a) PC1 altered the aspect ratio of the scapular body. (b) PC2 shows a change from cranial to lateral orientation of the glenoid as the shape moves from tear- to asymptomatic. (c) PC3 shifted the orientation and position of the acromion and coracoid process and was not associated with tears. (d) PC4 shows an increase in the subacromial space and narrowing of the supraspinous fossa as the shape moves from tear- to asymptomatic.

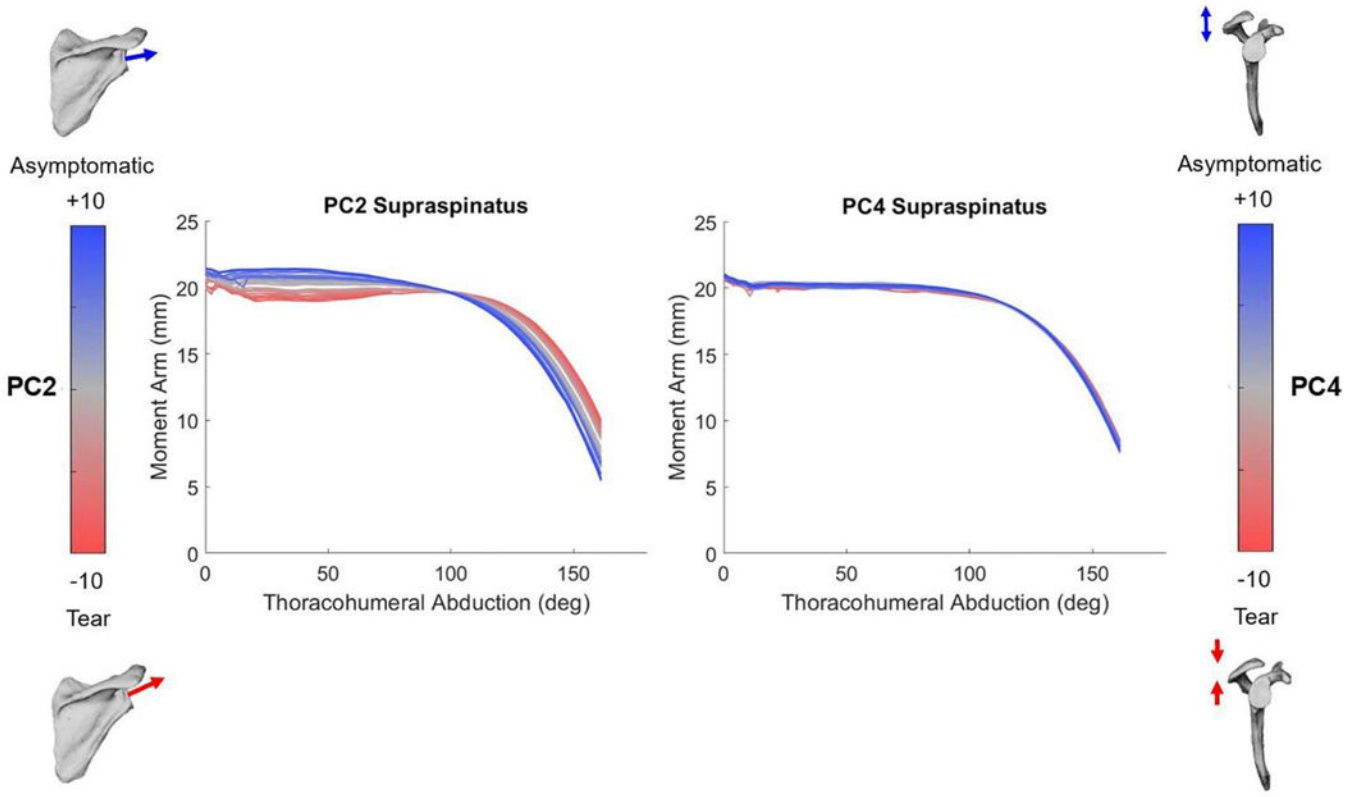

Fig. 6.

Supraspinatus moment arm curves for 160 degrees of thoracohumeral abduction. Moment arm curves for the 21 generated shape models are plotted for each principal component. The arbitrary scale of −10 to +10 spans the range of the PC scores calculated in the dataset, where a negative score is associated with the tear subjects and a positive score is associated with the asymptomatic subjects.

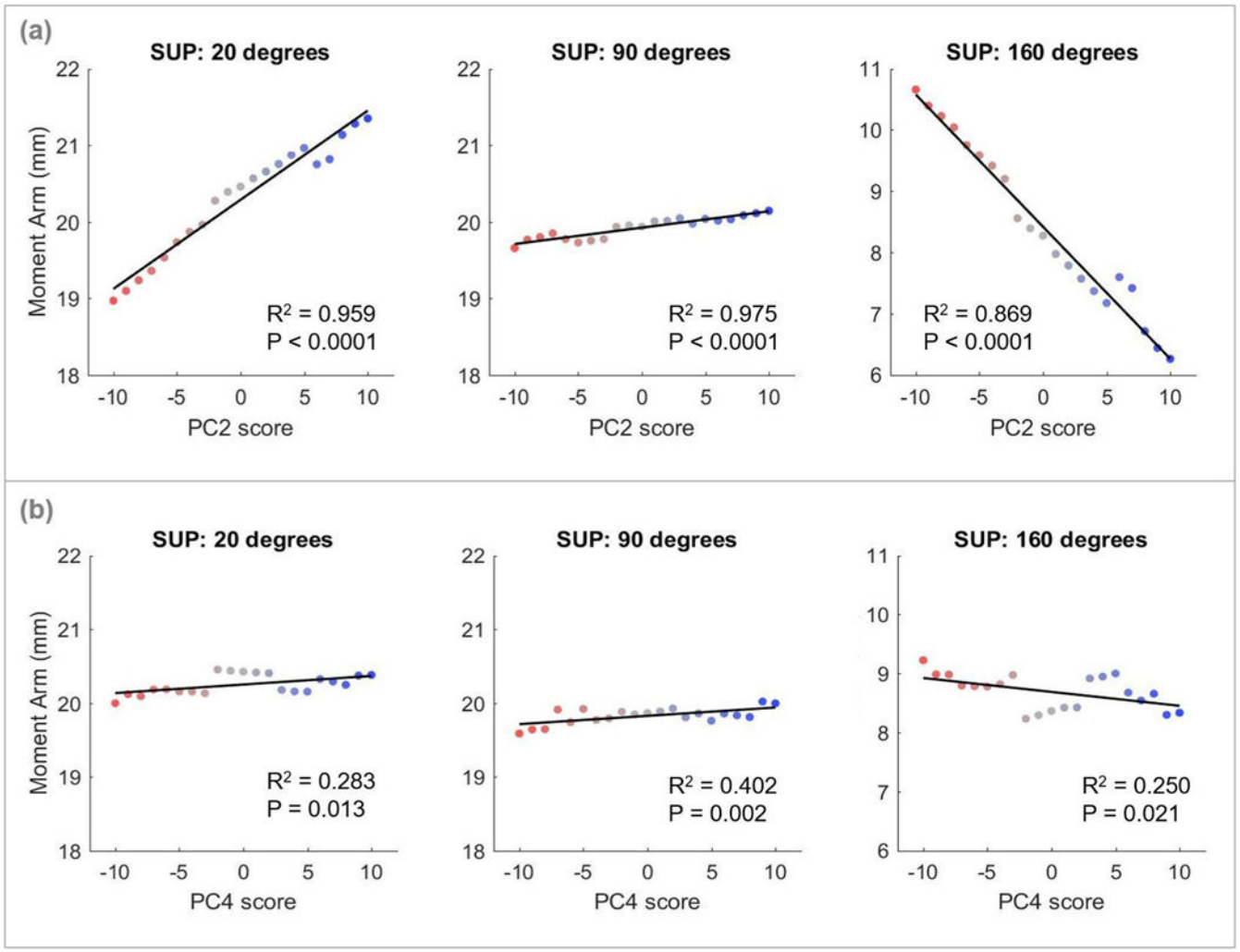

Fig. 7.

Supraspinatus abduction moment arms at 20°, 90°, and 160° of abduction for scapular shape models generated across (a) PC2, representing change from cranial to lateral orientation, and (b) PC4, representing change from small subacromial space to large subacromial space. R^2 and *P* values are shown for the results of the statistical analysis.